

Arthrospira Platensis Mediated Green Biosynthesis of Silver Nanoparticles as Breast Cancer Controlling Agent: In-vitro and In-vivo Safety Approach.

Nehal El Deeb (✉ nehalmohammed83@gmail.com)

City of Scientific Research and Technological Applications

Mai A. Abo-Eleneen

Tanta University Faculty of Science

Omyma A. Awad

Tanta University Faculty of Science

Atef M. Abo-Shady

Tanta University Faculty of Science

Research Article

Keywords: Green synthesis, AgNPs, Anti-proliferative, Anticancer, Breast cancer

Posted Date: August 9th, 2021

DOI: <https://doi.org/10.21203/rs.3.rs-769698/v1>

License:  This work is licensed under a Creative Commons Attribution 4.0 International License.

[Read Full License](#)

Abstract

Biogenic Silver Nanoparticle (bio-AgNPs) is one of the most fascinating nanomaterials used in the biomedical purposes. In the current study, we biosynthesized AgNPs (bio-AgNPs) using *Arthrospira platensis*(A-bio-AgNPs), *Microcystis aeruginosa*(M-bio-AgNPs)and *Chlorella vulgaris*(C-bio-AgNPs) active metabolites and evaluated their anticancer efficacy against breast cancer. The recovered bio-AgNPs were characterized using Scanning and Transmission Electron Microscopy (SEM and TEM) and their safety profiles were monitoring *in-vitro* on PBMCs cells and *in-vivo* on Albino mice. The obtained results indicated the safety usage of bio-AgNPs at concentration of 0.1 mg/ml on PBMCs cells and 1.5mg/ml on the Albino mice. The bio-AgNPs displayed dose-dependent cytotoxic effects against HepG-2, CaCO-2 and MCF-7 cell lines by inducing ROS and arresting the treated cells in G0/G1 and sub G0 phases. In addition, A-bio-AgNPs induced breast cancer cellular apoptosis by down regulating the expression of survivin, MMP7, TGF and Bcl2 genes. Upon A-bio-AgNPs treatment, a significant reduction in tumor growth and prolonged survival rates were recorded in breast cancer BALB/c model. Furthermore, A-bio-AgNPs treatment significant decreased theKi 67 protein marker from 60% (in the untreated group) to 20% and increased Caspase 3 protein levels to 65% (in treated groups) comparing with 45% (in Doxorubicin treated groups).

I. Introduction

Cancer is a life-threatening disease and leads the cases of deaths around the world. According to the WHO, the annual cancer cases are to rise from 14 million in 2012 to 22 million in the next two decades (McGuire 2016). Thus, searching for potent effective and safe anticancer drugs is one of the most influenced objectives[1]. Among the various approaches, the exploitation of nanotechnology is one of the most effective approaches to recognize different hits and leads [2]. In nanomedicine field, there are great interest in the synthesis of metal nanoparticles as gold and silver to be as anticancer agents [3, 4]. Because of their distinct characters and promising applications in the medical fields as anticancer and antimicrobial, silver nanoparticles AgNPs are widely used [5]. There are three methods used in the preparation of nanoparticles; physical, chemical and biological synthesis [6]. Green synthesis method is ultimately superior because of a multitude of reasons to begin with saving highly expensive chemicals and energy another reason is that the produced nanoparticles are preferred more than the nanoparticles manufactured with both chemical and physical methods finally this green method is eco-friendly [7]. Plants, bacteria, fungi, algae, etc. are widely used in nanoparticles green synthesis [8,9]. In their extracts, various bioactive compounds found, as proteins/enzymes, amino acids, polysaccharides, polyphenols, aldehydes and ketones that acting as ions reducing and stabilizing agents during the nanoparticles production process to form the favorite shapes and sizes [10]. Among the microorganisms, microalgae have a wonderful part in nanoparticles preparation and metals toxicity bioremediation and their biotransformation to altered nontoxic materials [11,12]. Unlike the most reported microorganisms that used in AgNPs biosynthesis, blue green algae (Cyanobacteria) were used as nonpathogenic microorganisms that used in its biosynthesis, *Spirulina platensis*, is an important example of these

microorganisms. *Arthrospira (Spirulina)* is filamentous cyanobacterium (Oscillatoriaceae) and shows great plasticity because it has a soft cell wall made of complex sugars and protein [13], they occur naturally in tropical and subtropical lakes at high pH and high carbonate and bicarbonate concentrations. In present study, we test the ability of *S. platensis* cell-free supernatant to form AgNPs in an aqueous system and investigate their anticancer effects against breast cancer. Moreover, we obtained preliminary visions on the molecular anticancer mechanisms against breast cancer using *in-vitro* and *in- vivo* breast cancer model.

II. Methods

II.1. Green synthesis and characterization of silver nanoparticles (bio-AgNPs) using algal free culture.

- **Algal strains and culture conditions.**

Chlorella vulgaris was cultured on Kuhl's medium for 20 days at 25 ± 2 °C and 200 LUX, *Arthrospira platensis* was cultured on modified Zarrouk medium for 16 days at about 27 ± 2 °C and 2500 while *Microcystis aeruginosa* was cultured on BG11 for 16 days at about 27 ± 2 °C and 2500 LUX, algal cultures shacked twice per day.

- **Green synthesis of bio-AgNPs.**

Fifty ml of AgNO₃ (1Mm) were drop wisely added to 50 ml of each culture filtrate of *A. platensis* (PH = 11), *M. aeruginosa* (PH = 6) and *C. vulgaris* (PH = 6.6). Each preparation was shacked for 1 hour (220 rpm) at room temperature. The formed pellets were collected by centrifugation at 10000 rpm for 10 min and then washed 3 times with distilled water before drying and storing at room temperature till use.

- **Bio-AgNPs characterization.**

Scanning Electron Microscopy (SEM).

The microstructures and morphology of the bio-AgNPs particles were observed using a Joel 6360LA scanning electron microscope (JEOL Ltd., Tokyo, Japan) at an accelerated voltage of 15 kV. The samples were mounted on the specimen holder with double sided adhesive tape, after gold coating using a JFC-1100E sputter (JOEL Ltd., Tokyo, Japan), the images were captured using an accelerating voltage of 15 kV.

Transmission Electron Microscopy (TEM).

The collected bio-AgNPs pellets were dispersed in distilled water and their microstructures were studied with a Joel 6360LA transmission electron microscope (JEOL Ltd., Tokyo, Japan), by double sided adhesive tape. A thin film of sample was prepared by placed 5 µl of the collected bio-AgNPs on a carbon coated 3-mm copper grid that dried at room temperature. ImageJ software was used for examination and poly dispersity index was calculated according to the following equation:

Loading [MathJax]/jax/output/CommonHTML/jax.js

$$\text{PolyDispersityIndex(PDI)} = \left(\frac{\text{StandardDeviation}}{\text{MeanDiameter}} \right)^2$$

II.2. In-vitro safety assay and anticancer effects of bio-AgNPs.

- **Safety assay of bio-AgNPs on Peripheral Blood Mononuclear Cells (PBMC).**

For the determination of *Chlorella vulgaris* (C-bio-AgNPs), *Microcystis aeruginosa* (M-bio-AgNPs) and *Arthrospira platensis* (A-bio-AgNPs) non-toxic dose which does not display toxic effects on PBMC cells, the cytotoxicity assay was accomplished using MTS assay. 100µl of PBMCs suspension (6×10^4 cell/ml) was seeded in 96-well plates. The seeded plates were incubated at 37°C in humidified 5% CO₂ for 24 hr. After incubation, the exhausted old medium was replaced with either 100 µl of treatment concentrations (prepared in culture medium) or medium (negative control). The plates were incubated at the same growth conditions for 3 days after that, the cytotoxic effects were quantified using MTS assay Kit according to the instruction protocol.

- **In-vitro anticancer activity of bio-AgNPs against HepG-2, CaCO-2 and MCF-7 cell lines.**

The anticancer activities of C-bio-AgNPs, M-bio-AgNPs and A-bio-AgNPs were quantified against HepG-2, CaCO-2 and MCF-7 cell lines using MTS assay as described above.

- **Selectivity index.**

The selectivity index of the recovered bio-AgNPs to cancer cells was quantified according to Koch et al.[14] protocol with a minor modification, where; SI = IC_{50nc} / IC_{50cc}, where IC_{50nc} refers to the IC₅₀ value of the tested compound on normal cells while; IC_{50cc} refers to the IC₅₀ of the tested compound on cancer cell line.

II.3. The mode of anticancer action of the bio- AgNPs.

- **Intracellular reactive oxygen species induction using bio-AgNPs.**

The total induced intracellular ROS by C-bio-AgNPs, M-bio-AgNPs and A-bio-AgNPs were detected in PBMC using 2, 7-dichloro dihydrofluorescein diacetate (H₂DCF-DA) and flow cytometry. DFCH-DA enters cells and further oxidized by ROS forming fluorescent product 2',7'-dichlorofluorescein (DCF). Briefly, PBMC cells were grown in 96 well plates for 24 hrs, 100 µl of bio-AgNPs non-toxic doses were added to cells and incubated for 24 hrs. After that, cells were incubated with H₂DCF-DA at a final concentration of 50 µM for 30 min. In the positive control group, ROS was induced by loading cells with *E. coli* LPS (lipopolysaccharide 100 ng/ml) in RPMI. After 1 h incubation, the stimulants were discarded and cells were washed three times with pre warmed PBS, all samples were analyzed using a BD FACSC calibur flow cytometer with Cell Quest software. For quantification of DCF fluorescence, at least 10,000 events were used for each measurement [4].

- **Cell cycle analysis.**

The alterations of HepG-2, CaCO-2 and MCF-7 cell cycle pattern upon A-bio-AgNPs treatment were determined using flow cytometry (Léonce et al. 2001) in which PI was used as cellular stain that discriminates living cells from dead cells. After treatment, cell suspensions were stained with 0.5 mL of warm PI solution (7 ml of PI solution consists of 0.35 ml of PI solution (1 mg/ml), 0.7 ml RNase A solution (1 mg/ml), and 6 ml of PBS). All samples were kept on ice until flow cytometric analysis.

- **Apoptosis and necrosis assessment.**

Acridine orange/ethidium bromide (AO/EB) assay was used to differentiate between Apoptosis and necrosis cellular status.

Acridine orange could stain both live and dead cells while; ethidium bromide stain only cells that have lost membrane integrity. After A-bio-AgNP treatment, MCF-7 cell suspension (0.5×10^6 cells/ml) was incubated with 1 μ l of AO/EB solution and aliquot of cell suspension was examined using a fluorescence microscope [15].

- **Bio-AgNPs regulate MCF-7 oncogenes and tumor suppressor genes.**

The molecular anticancer action of A-bio-AgNPs was explained by studying their effects in controlling the expressions of p53, Bcl2, MMP7 (metalloproteinase-7), TGF α (Transforming growth factor) and Survivin genes in MCF-7 treated cells. After 24 hrs cellular treatment with sub-IC50 concentrations, RNA was extracted using the Qiagen RNA Kit. cDNA was synthesized using r First Strand cDNA Synthesis Kit (Roche) and Real-time qPCR was conducted using primer sets listed in Table (S1) and SYBR Green Master Mix (Applied Biosystems). The gene expression levels were calculated and normalized using b-actin and expressed as a fold change compared with control. The obtained results were analyzed using a CFX-96 (Bio-Rad).

II.4. Safety assay and anticancer effects of A-bio-AgNPs, *In-vivo*.

Based on the *In-vitro* studies, A-bio-AgNPs was selected to complete the all *in-vivo* experiments due to its anticancer efficacy.

- **In-vivo safety assay.**

BALB/c mice (35–45 gm) were purchased from VACSERA, Cairo, Egypt. After one week adaptation, the experimental animals were divided into three groups, each one contained 5 male albino mice (35–45 gm).

The *in-vivo* protocols were reviewed and approved by Medical Research Institute, Alexandria, Egypt, Animal Care and Use Committee.

- **Experimental design.**

In the first group, mice were intraperitoneally injected (IP) with A-bio-AgNPs (0.3mg/ml, 7µg/g body weight). IN the second group mice; mice were IP injected with 0.15mg/ml A-bio-AgNPs (3.5µg/g body weight). The last group was represented the untreated control one which injected with 9% saline. After 2 weeks and upon scarifying, serum samples were collected and the the blood biochemical tests were performed. Serum alanine aminotransferase,Aspartate aminotransferase, Alkaline phosphatase (ALP) activities, total protein, albumin concentration, Urea and creatinine concentrations were determined using Bio diagnostic kit, Egypt according to its manual instruction.

- **In-Vivo anticancer effects of A-bio-AgNPs treatments.**

Mice were subcutaneously injected with 2 X10⁵ of Ehrlich Ascites Carcinoma cells (Ehrlich cells, EAC) in the right flank of BALB/C. After 5 days of tumor induction, the tumor burdens were measured by Vernier caliper. Mice were then grouped based on measurements into four groups, each group was adjusted to contain the same average of tumor burden mice and each one contained 5 female mice (22–28 gm).

After 7 days of tumor induction, In the first group: 5 tumor bearing female mice were IP injected with 0.15 mg/ml of A-AgNPs (3.5gm/Kg body weight). In the second group, another 5 tumor bearing mice were injected locally (intertumoral injections) with 0.15mg/ml A-AgNPs (3.5gm/Kg body weight). In the positive control group, 5 tumor bearing mice were IP injected with Doxorubicin (0.15mg/ml; 3.5gm/Kg body weight). Also, 5 tumor bearing (female) mice were IP injected with 9% saline (negative control group). All mice bearing Ehrlich Ascites Carcinoma were treated 3 times on day 7, 10 and 17. The tumor measurements were performed every 2 days and calculated as tumor volume = (width² × length)/2 as reported [16]. Animals were checked until they reached the killing criteria (tumor burden reached 10% of body weight, the presence of tumor ulceration or mice became dying).

The study lasted for 1 month before scarifying under diethyl ether anesthesia, serum samples, tumors tissue and different organs were collected for blood biochemical assays and histopathological examinations.

- **Histopathology and Immunohistochemistry studies.**

After mice scarifying, one longitudinal half of each organ was fixed at 10% formalin for the histopathological analysis. The obtained sections were stained with hematoxylin and eosin (H&E), microscopically examined for the presence edema, erosion and necrosis.For immunohistochemical analysis, 3 µm sample sections were deparaffinized with xylene and ethanol, the intrinsic peroxides activity in tissue sections was blocked with Peroxidase. After protein blockage, the prepared sections were incubated with anti-Ki 67 and anti-Caspase 3 antibodies [17] for 30 minutes then, washed for 5 minutes two times in PBS. Mayer's hematoxylin was used to counter stain the slides. The stained sections were examined under a light microscope (Olympus BX53, Tokyo, Japan).

11.5. Statistical analysis

Loading [MathJax]/jax/output/CommonHTML/jax.js

All results are presented as mean \pm SD (standard deviation) of three replicates and the statistical analyses were carried out using SAS program. Data obtained were analyzed statistically to determine the degree of significance between treatments using one- and two-way analysis of variance (ANOVA) at $P \leq 0.005$ (SAS program 1989–1996). IC50 values and the statistical analysis of cytotoxicity and safety assay experiments were carried out using GraphPad prism 8.

iii. Results

III.1. Green Synthesis and characterization of silver nanoparticles.

- **Culturing and growth curves of *C. vulgaris*, *A. platensis* and *M. aeruginosa*.**

Algal species growth was measured as optical density (O.D) every two days to determine the maximum growth of each different organism. The obtained data indicated that *A. platensis* and *M. aeruginosa* optimum growth were recorded upon culturing for 16 days on modified Zarrouk medium and BG11, respectively at $27 \pm 2^\circ\text{C}$ and 2500 LUX (Fig S1, a and c). While *C. vulgaris* maximum growth was recorded after culturing on Kuhl's medium for 18 days at $25 \pm 2^\circ\text{C}$ and 4000 LUX (Supplementary Fig S1b).

- **Silver nanoparticles green Synthesis and characterization.**

Silver nanoparticles (bio-AgNPs) were biosynthesized using cell free supernatants of *C. vulgaris*, *A. platensis* and *M. aeruginosa*. The supernatants of *A. platensis*, *M. aeruginosa* and *C. vulgaris* were collected at the growth stationary phases after 10, 12 and 16 days, respectively (Fig S1b). The biologically active compounds of algal filtrates acted as silver ion reducing agents. The primary analysis was done via the observation of color change from colorless to brown that confirmed the formation of bio-AgNPs (comparing with silver nitrate aqueous solution that remained colorless). Furthermore, both Scanning (SEM) and transmission (TEM) electron microscope analysis proved the spherical shapes of the recovered bio-AgNPs with size ranged from 9 to 17nm (Fig. 1,2.)

III.2. In-vitro safety assay and anticancer effects of bio-AgNPs.

- **Safety patterns of bio-AgNPs.**

The safety usage of the bio-AgNPs was tested on normal mammalian cells, Human peripheral blood mononuclear cells (PBMC), using bio-AgNPs different concentrations from 0.125 to 4 mg/ml. After treatment, cellular viability was quantified using MTs assay (Fig S2). The results revealed the nontoxic dose of M-bio-AgNPs, C-bio-AgNPs and A-bio-AgNPs on PBMC cells that recorded 0.1 mg/ml, this nontoxic dose showed 0.3, 14.2 and 16.9% cellular viability inhibition, respectively. So, bio-AgNPs at 0.1 mg/ml was selected to complete the *in-vitro* studies.

III.3. Anticancer activities of the bio-AgNPs against HepG-2, CaCO-2 and MCF-7 cancer cells.

Loading [MathJax]/jax/output/CommonHTML/jax.js

The anticancer effects of bio-AgNPs were done against 3 different cell lines using MTS assay. In general, all bio-AgNPs showed great abilities to inhibit cancer cells proliferations with percentages exceeded 95%. Upon treating cells with the non-toxic bio-AgNPs dose (0.1 mg/ml), A-bio-AgNPs was the most potent treatment against HepG-2, CaCO-2 and MCF-7 cells with inhibition percentages of 86.2, 94.2 and 96.6, respectively (Fig. 3, a, b,c). In addition, A-bio-AgNPs IC50 values reached 7.8, 14.2 and 5.9 µg/ml against HepG-2, CaCO-2 and MCF-7 cells, respectively (Fig. S3a). Furthermore, A-bio-AgNPs showed great abilities to inhibit MCF-7 cells with selectivity index exceed 1847 followed by the same treatment on HepG-2 cells with 1406.44 selectivity index. Also, M-bio-AgNPs showed massive toxic effects against CaCO-2 cells with selectivity index 860.93 (Fig. S3 b).

Furthermore, the morphological characters A-bio-AgNPs-MCF-7 treated cells showed the appearance of undergoing apoptotic cells that characterized by cellular rounding up, shrinkage, membrane blebbing and loss of cell adhesion. (Fig. S4).

III.4. The mode of anticancer action of the bio- AgNPs.

- **Induction of cellular ROS.**

The intracellular ROS in PBMCs by bio-AgNPs treatment were quantified using flowcytometry and compared with LPS (positive control). The maximum induced ROS percentage (Fig. 4) was recorded upon PBMCs treatment with M-bio-AgNPs (50.16) followed by A-bio-AgNPs and C-bio-AgNPs (46.3 and 40, respectively) comparing with both negatively controlled cells (16.35) and positively LPS induced cells (19.51).

- **Cell cycle analysis.**

The cell cycle phases distribution of HepG-2, Caco2 and MCF-7 cells after the treatment with A-bio-AgNPs were done by comparing the phases of treated cells with those of the untreated cells. After HepG-2 treatment with A-bio-AgNPs, the cells population in subG0 phase (apoptotic cells) were increased by about 1.3% over the untreated cells percentage to record 35.6% (Fig S4 a). While, upon CaCO-2 cells treatment, the treated cells were arrested in S phase with percentage 66.4 (Fig S5 b). On the other hand, the A-bio-AgNPs treatment causing G0/G1 phase arrest in MCF-7 cell with percentage 61.6 (Fig S5c).

- **Gene expression patterns of bio-AgNPs-treated cancer cells.**

The possible mechanisms of AgNPs-mediated cell death action via the apoptotic regulators have been confirmed via gene expression analysis. gene expression levels of Bcl2, Survivin, MMP7, P53 and TGF were quantitatively measured by RT-PCR after β actin normalization (Fig. 5). The overall results indicated that, comparing with the untreated cells, A-bio-AgNPs treatment induced cellular apoptosis in breast cancer cells via the down regulation of survivin, MMP7, TGF and Bcl2 genes expressions. While C-bio-AgNPs induced MCF-7 cellular apoptosis via MMP7 gene down regulation and P54 gene up-regulation. Furthermore, upon MCF-7 cells treatment with M-bio-AgNPs, cell apoptosis induction verified via survivin

- **Induction of Apoptosis and necrosis.**

The all above results indicated the potent anticancer effects of A-bio-AgNPs against all cell lines while, MCF-7 cells were the most sensitive cells to the treatment. So, in the following section we will evaluate the efficacy of A-bio-AgNPs against breast cancer models.

Nuclear changes during apoptosis were visualized via fluorescence microscope using acridine orange/ethidium bromide (AO/EB) staining. In the living cells, nuclei appeared with normal green staining with green chromatin and they showed organized structures, while in the early apoptotic stage, cells exhibited condensed or fragmented chromatin (green or orange). Nevertheless, during late apoptotic or necrotic stages, cells have displayed similar normal nuclei staining, as live cells, but with orange chromatin. Upon MCF-7 cellular treatment with A-bio-AgNPs, the treated cells appeared with an early apoptotic feature with orange-stained multinucleated cells (Fig. 6).

III.5. In-vivo safety assay and anticancer effects of A-bio-AgNPs.

- **In-Vivo safety assay.**

Upon our previous experiment, the safety usage of A-bio-AgNPs was tested on BALB/c mice using two doses (3 and 1.5 mg/ml). The results indicated that, the first group that treated with 3 mg/ml of bio-AgNPs showed significant elevation in the serum concentrations of ALT and AST. While the group that injected with 1.5mg/ml of bio-AgNPs didn't record significant differences from control group. Also, the animal group that treated with 1.5mg/ml of A-bio-AgNP didn't showed any significant differences from the control group in the concentration of serum protein, albumin and creatinine and with slightly elevation in the concentrations of serum urea and bilirubin (Data not shown).

- **In-vivo antitumor effect of the A-bio-AgNPs.**

To confirm the obtained antitumor effects of A-bio-AgNPs, AgNPs were injected into BALB/C mice via two routs (Fig. 7a).; I.P and SC. Injection with 0.15mg/ml and 3.5gm/Kg body weight. Mice body weight results during 30 days of the experiment showed dramatically weight loss over the first days of tumor progression, then a significant increase in the body weight was recorded after all treatment regimens (Fig. 7b). Also, the tumor size increased intensively over the first days of the experiment then, the growth started to be inhibited obviously after all treatments(Fig. 7c). All treatments are able to induce a great delay in tumor growth and prolonged survival in mice without significant differences among them. The highest inhibition of tumor growth was recorded in the group that treated intratumorally with A-bio-AgNPs followed by that treated intraperitoneally. Also, the results of red blood cells (RBCs), White blood cells (WBCs) and platelets counts were recorded in all animal groups (Fig. 7D). Comparing with the control group, the DOX treated-mice showed the lowest counts of blood cells; 5.7×10^3 cells/ μ L of RBCs, 3.46×10^3 cells/ μ L of WBCs and the platelet counts reached 1.1×10^3 cells/ μ L. The tested mice in all groups were seen with distress marks (weight loss; dehydration; rapid or shallow breathing; hunched

posture/immobility; piloerection; guarding behavior; bleeding from any orifice; death). All mice in the bio-AgNPs groups tolerated the used dose with no appearance of toxicity/or mortality.

The histopathological examination results of the DOX., PBS and bio-AgNP treated mice indicated the presence of viable tumor and necrotic areas in all samples with a smaller number of malignant, advanced necrotic and fibrotic cells in the A-bio-AgNPs treated groups (Fig. 8a). The tissue sections of the control group indicated malignant cells, increased N/C ratio, loss of cell architecture and necrosis and metastasis in the lipid layer (Fig. 8a). While in the animal groups which treated with DOX., the breast tissue section showed fibrotic reactions, advanced necrosis, less malignant viable cells (Fig. 8a).

- **Immunohistochemistry (IHC).**

Immunohistochemistry allows the evaluation of proteins localization in the context of tumor structure. Ki67 is a nuclear antigen present in mid G1, S, G2, and the entire M phase of the cell cycle, it serves as a proliferation marker. Our results confirmed the presence of Ki 67 marker in the tumors bearing un-treated mice (appeared as brown color spots) with percentage 60%. This percentage was highly reduced to be 20% in the A-bio-AgNPs treated mice (injected in solid tumors). While, in the Doxorubicin treated group, Ki 67 protein levels in tumors sections of A-bio-AgNPs (I.P injected)-treated mice was less than it (8%, Fig. 8b).

on the other hand, the activated caspase-3 and caspase-7 can cleave multiple structural and regulatory proteins, which are critical for cell survival and maintenance. On contrary with the previous results, Caspase 3 protein (the apoptotic biomarker) in the tumor sections of untreated mice was almost absent while, it was increased with nearly 25% in the tumor sections of mice treated with A-bio-AgNPs (injected in solid tumors). The highest levels of Caspase 3 protein were observed in the groups that intraperitoneally treated with A-bio-AgNPs with percentage 65% comparing with 45% in Doxorubicin treated groups (Fig. 8c).

Iv. Discussion

Breast cancer is a major ongoing public health matter among women in both developing and developed countries. In the past decades, there were strong improvement in the development of breast cancer treatment. Nevertheless, the existing clinical lines are invasive with low specificity and lead to severe side effects. The rapid development of nanotechnology in medical fields strongly supported human cancer diagnosis and treatment fields. Nanoparticles-based strategies could overcome the cellular barriers and permits sustained blood circulation period, more tumor targeting and improved the drugs-tumors accumulation [18, 19]. There are various nanomedicines that approved by the US FDA or under different stages of development in clinical trials as breast cancer therapeutics as; Abraxane, Nanoparticle albumin-bound paclitaxel, that approved in 2005 [20, 21] or non-approved yet as tamoxifen/AgNPs dual core-folate decorated shell [3]. In the nanomedical field, the selected biomaterials should be systemically nontoxic and biocompatible [22] to be approved in cancer treatment. So, we focused on the green

Loading [MathJax]/jax/output/CommonHTML/jax.js AgNPs using microalgal extracts with size ranged from 9-

17nm with anti-cancer properties. Various studies indicated the successful role of different cyanobacterial filtrates in the biosynthesis of AgNPs [23–26]. Mahdiah et al. [27] explained that, iron nanoparticles formation is due to ion reduction to metal nanoparticles by algal extracellular reductase that secreted in the cell free supernatant. In addition to the algal extracellular reductase, Hamouda et al. [23] clarified the role of algal extracellular proteins of *Oscillatoria Willei* NTDM01 as a capping agent in the formation of spherical AgNPs (100–200 nm). The algal extracellular proteins or polysaccharides could bind to the nanoparticles either through free amine groups or [28] cysteine residues [29, 30]. In addition to the synthesis of suitable anticancer, the safety usage and the limit adverse effects of any newly tested drugs in parallel with drug efficacy are the main important issues in the success of their approval as therapeutic agents. So that, our safety usage assessment of the bio-AgNPs were confirmed at both *in-vitro* and *in-vivo* levels. Our results indicated that, on PBMC cells, the nontoxic doses of bio-AgNPs that synthesized by *Microcystis aeruginosa*, *Chlorella vulgaris* and *Arthrospira platensis* filtrates were 0.1 mg/ml which showed cellular viability inhibition percentages 10.3, 14.2 and 16.9, respectively. While another study by Yang et al. [31] tested the cytotoxic effects of AgNPs with different sizes (5 nm, 28 nm and 100 nm) on PBMCs, they indicated that, the nontoxic doses of AgNPs ranged 0.15 to 0.3 µg/ml which is much closed to our finding. Furthermore, other studies investigated the cytotoxic effects of the biogenic O-AgNPs on human erythrocytes integrity [23]. Hamouda et al. [23] clarified that, by using AgNPs at concentrations, 0.5, 5.0, 7.5, 10 µg/ml showed cell lyses as 0.45, 0.76, 1.03, 1.68%, respectively on blood cell culture. The cellular toxicity mode of actions of AgNP were mainly based on their physico-chemical characters as shape, charges, sizes, stabilization and presence of other capping molecules with the type of the targeted cells so that, the nanoparticles toxicity must be checked on different cell types [32–35]. In context, the capping process of AgNPs with certain polymers or polysaccharides at definite concentrations showed a promising biological activity without any cytotoxic effects with that effective dose (Liu et al. 2012), these findings could explained the safety usage of our prepared bio-AgNPs. At the *in-vivo* level, spleen, liver and kidney are the most affected organs to AgNPs toxicity (their negative effects include ROS induction, pathological changes in liver morphology, and enzyme activity) with less distribution profile in the other organs [36, 37]. However, our previous data (supplementary file) showed that, the intraperitoneal injection of *Arthrospira* bio-AgNPs at 1.5 mg/Kg into Albino mice didn't record any significantly effects on the liver or kidney functions. Again, this non cytotoxic effects could be explained by a study of Ashraf et al. [38], they explained that AgNPs green synthesis approach provide advanced direction for NPs synthesis without using toxic reductants and stabilizers, which mean more safety and less cytotoxic effects. Concerning with the anticancer efficacy of AgNPs, many recent studies reported the anticancer effects of AgNPs against different cancer cell lines as breast [3, 39], ovary [40], brain [41, 42], cervix [43], liver [44], colon [45, 19], lung [46], pancreas [47], and blood [48–50]. At the *in-vitro* level, Swanner et al. [39] reported that, the non-toxic doses of AgNPs (tested on the non-cancerous cell lines and normal cells; Kidney, liver and monocytes) were toxic to 3 different triple negative breast cancer cell lines. In this context, our obtained results proved the anticancer effects of *Arthrospira*-bio-AgNPs against HepG-2, CaCO-2 and MCF-7 cells with inhibition percentages 86.2, 94.2 and 96.6, respectively. Furthermore, this treatment showed 1847.05 selectivity index against MCF-7 cells. In order to explain the

Swanner et al. [39] explained that, MDA-MB-231 breast cancer cells treated with AgNPs at dose 37.5 µg/mL reduce cell number in G0/G1 phase with an increase and cell cycle arrest in S-phase cells. In the same context, our obtained results indicated that after AgNPs treatment, the treated CaCO-2 cell arrested in S phase and MCF-7 cell cycle arrested in G0/G1 phase with cells population increasing in subG0 phase. Furthermore, recent research was explained another key role in the AgNPs anticancer effects against different cancer cell this factor is the cellular redox balance and ROS [3, 51]. Our quantified ROS results indicated a significant induction in the intracellular ROS using all tested bio-AgNPs comparing with both positive (LPS induced) and negative PBMCs control cells. In addition to ROS induction and the alteration in cell cycle pattern, our results indicated that, the tested bio-AgNPs cytotoxic effects against breast cancer cells could be explained via MMP7, TGF and Bcl2 genes down regulation. There are few reports that tried to clarify the role of AgNPs as a regulatory agent in cancer cell apoptotic or proliferative pathways. Our previous work [19] clarified that, the biogenic AgNPs that synthesized by *Balanites aegyptiaca* saponins showed anticancer effects *in-vitro* against colon and liver cancer cells by the downregulation of MMP7, BCL2 and up-regulation of IKaB. The mode of action of AgNPs embedded with *Arthrospira* extracts to inhibit MFC-7 proliferation was explained through BCL2-caspase cascade that mediated mitochondrial dysfunction complemented with TGF-b/MMp7 pathway [52]. These pathway combinations may be the cause of cytotoxic effects of AgNPs against MCF-7 even at lower concentration that explained by our mentioned results. For more explanation to the *Arthrospira*-bio-AgNPs mode of action at the *in-vivo* level, the immuno-histochemistry analysis of tumor bearing mice indicated that caspase 3 levels of control and treated mice were comparable with staining intensity varied from strong to weak. Caspase 3 is considered as the most important part of cellular apoptotic pathway; caspase 3 active form levels has been checked in different cancer types in relationship with histological grade of malignancy and could be used as patient's overall survival prognostic marker [53]. The current study indicated the potentialities of AgNPs to induce cell death through caspase-dependent pathways activation that recorded from an elevation in caspase3 level in the treated group. The activated caspase that recorded in *Arthrospira*-bio-AgNPs treated groups could be resulted from the initiation of silver ions from AgNPs that induce oxidative stress that in turns activate caspase 3 [54]. The same findings were recorded by Urbańska et al. [55], they indicated that caspase 3 levels in AgNPs treated glioblastoma multiform *in-vivo* model looked to be on the border between the spontaneous and the induced apoptosis. Interestingly, our current results showed that *Arthrospira*-bio-AgNPs treatment was highly reduced Ki-67 percentage from 60–20% in the mice tumor sections. Ki-67, proliferation marker, is the most controversially used parameter in breast cancer treatment and diagnosis [56]. Ki-67 antigen is expressed in S, G1, G2 and M cell cycle phase [57] that mean upon treatment, the Ki-67 antigen reduction could arrest cell cycle in the one of the above-mentioned phases. This finding supported our previously mentioned results that MCF-7 cell cycle arrest in G1 phase upon *Arthrospira*-bio-AgNP treatment which resulted in Ki-67 antigen reduction in the tested tissues. The all above explained factors could be illuminated the mode of anticancer actions of Bio-AgNPs against breast cancer. Finally, we concluded that, Algal-mediated synthesis of silver nanoparticles using the extract of *Arthrospira platensis* promotes green nanotechnology. The current study showed the cytotoxic effects of A-bio-AgNP against breast

cancers at both *in-vitro* and *in-vivo* compared to the standard doxorubicin. The A-bio-AgNP treatment at the nontoxic doses provides a novel alternate or complementary approach in breast cancer treatment.

Declarations

- **Funding information**

This research did not receive any specific grant from funding agencies in the public, commercial, or not-for-profit sectors.

- **Conflict of interest**

The authors declare that they have no conflict of interest.

- **Author contributions**

Nehal: designing of the work, the acquisition, analysis, interpretation of data, drafted the work and substantively revised.

Mai: Helped in the acquisition, analysis, interpretation of data, drafted the work.

Omyma and Atef: Supervised, revised and approved the submitted version.

- **Ethical statement.**

All *in-vivo* studies were done according to City of Scientific Research and Technological Applications, Egypt guidelines. The Research Ethical Committee at the pharmaceutical industries center, Egypt under international and institutional guidelines (REC-FPTU) approved all used experimental protocols.

- **Data availability statement**

All data generated or analyzed during this study are included in this published article (and its supplementary information files).

References

1. Al-Madboly LA, El-Deeb NM, Kabbash A, Nael MA, Kenawy AM, Ragab AE (2020) Purification, Characterization, Identification, and Anticancer Activity of a Circular Bacteriocin From *Enterococcus thailandicus*. *Front Bioeng Biotechnol* 8:450 doi:10.3389/fbioe.2020.00450
2. Chenthamara D, Subramaniam S, Ramakrishnan SG, Krishnaswamy S, Essa MM, Lin F-H, Qoronfleh MW (2019) Therapeutic efficacy of nanoparticles and routes of administration. *Biomaterials Research* 23(1):20 doi:10.1186/s40824-019-0166-x
3. Ibrahim OM, El-Deeb NM, Abbas H, Elmasry SM, El-Aassar MR (2020) Alginate based Loading [MathJax]/jax/output/CommonHTML/jax.js ated shell: Nanocomposite targeted therapy for breast cancer

- via ROS-driven NF- κ B pathway modulation. *Int J Biol Macromol* 146:119-131
doi:10.1016/j.ijbiomac.2019.12.266
4. Yassin AM, Elnouby M, El-Deeb NM, Hafez EE (2016) Tungsten Oxide Nanoplates; the Novelty in Targeting Metalloproteinase-7 Gene in Both Cervix and Colon Cancer Cells. *Appl Biochem Biotechnol* 180(4):623-637 doi:10.1007/s12010-016-2120-x
 5. Pugazhendhi A, Edison T, Karuppusamy I, Kathirvel B (2018) Inorganic nanoparticles: A potential cancer therapy for human welfare. *Int J Pharm* 539(1-2):104-111 doi:10.1016/j.ijpharm.2018.01.034
 6. Iravani S, Korbekandi H, Mirmohammadi SV, Zolfaghari B (2014) Synthesis of silver nanoparticles: chemical, physical and biological methods. *Res Pharm Sci* 9(6):385-406
 7. Saratale RG, Karuppusamy I, Saratale GD, Pugazhendhi A, Kumar G, Park Y, Ghodake GS, Bharagava RN, Banu JR, Shin HS (2018) A comprehensive review on green nanomaterials using biological systems: Recent perception and their future applications. *Colloids Surf B Biointerfaces* 170:20-35 doi:10.1016/j.colsurfb.2018.05.045
 8. Agarwal H, Venkat Kumar S, Rajeshkumar S (2017) A review on green synthesis of zinc oxide nanoparticles – An eco-friendly approach. *Resource-Efficient Technologies* 3(4):406-413 doi:<https://doi.org/10.1016/j.refit.2017.03.002>
 9. Elshinawy MI, Al-Madboly LA, Ghoneim WM, El-Deeb NM (2018) Synergistic Effect of Newly Introduced Root Canal Medicaments; Ozonated Olive Oil and Chitosan Nanoparticles, Against Persistent Endodontic Pathogens. *Front Microbiol* 9:1371 doi:10.3389/fmicb.2018.01371
 10. Rajan R, Chandran K, Harper SL, Yun S-I, Kalaichelvan PT (2015) Plant extract synthesized silver nanoparticles: An ongoing source of novel biocompatible materials. *Industrial Crops and Products* 70:356-373 doi:<https://doi.org/10.1016/j.indcrop.2015.03.015>
 11. El-Deeb NM, Abo-Eleneen MA, Al-Madboly LA, Sharaf MM, Othman SS, Ibrahim OM, Mubarak MS (2020) Biogenically Synthesized Polysaccharides-Capped Silver Nanoparticles: Immunomodulatory and Antibacterial Potentialities Against Resistant *Pseudomonas aeruginosa*. *Front Bioeng Biotechnol* 8:643 doi:10.3389/fbioe.2020.00643
 12. Igiri BE, Okoduwa SIR, Idoko GO, Akabuogu EP, Adeyi AO, Ejiogu IK (2018) Toxicity and Bioremediation of Heavy Metals Contaminated Ecosystem from Tannery Wastewater: A Review. *J Toxicol* 2018:2568038 doi:10.1155/2018/2568038
 13. Fujisawa T, Narikawa R, Okamoto S, Ehira S, Yoshimura H, Suzuki I, Masuda T, Mochimaru M, Takaichi S, Awai K, Sekine M, Horikawa H, Yashiro I, Omata S, Takarada H, Katano Y, Kosugi H, Tanikawa S, Ohmori K, Sato N, Ikeuchi M, Fujita N, Ohmori M (2010) Genomic structure of an economically important cyanobacterium, *Arthrospira (Spirulina) platensis* NIES-39. *DNA Res* 17(2):85-103 doi:10.1093/dnares/dsq004
 14. Koch A, Tamez P, Pezzuto J, Soejarto D (2005) Evaluation of plants used for antimalarial treatment by the Maasai of Kenya. *J Ethnopharmacol* 101(1-3):95-9 doi:10.1016/j.jep.2005.03.011
 15. Kasibhatla S, Amarante-Mendes GP, Finucane D, Brunner T, Bossy-Wetzel E, Green DR (2006) Acridine Loading [MathJax]/jax/output/CommonHTML/jax.js ning to Detect Apoptosis. *CSH Protoc* 2006(3)

doi:10.1101/pdb.prot4493

16. Jing Y, Tong C, Zhang J, Nakamura T, Iankov I, Russell SJ, Merchan JR (2009) Tumor and vascular targeting of a novel oncolytic measles virus retargeted against the urokinase receptor. *Cancer Res* 69(4):1459-68 doi:10.1158/0008-5472.Can-08-2628.
17. El-Seedi HR, El-Shabasy RM, Khalifa SAM, Saeed A, Shah A, Shah R, Iftikhar FJ, Abdel-Daim MM, Omri A, Hajrahand NH, Sabir JSM, Zou X, Halabi MF, Sarhan W, Guo W (2019) Metal nanoparticles fabricated by green chemistry using natural extracts: biosynthesis, mechanisms, and applications. *RSC Advances* 9(42):24539-24559 doi:10.1039/C9RA02225B
18. Tang X, Loc WS, Dong C, Matters GL, Butler PJ, Kester M, Meyers C, Jiang Y, Adair JH (2017) The use of nanoparticulates to treat breast cancer. *Nanomedicine (Lond)* 12(19):2367-2388 doi:10.2217/nnm-2017-0202
19. Yassin AM, El-Deeb NM, Metwaly AM, El Fawal GF, Radwan MM, Hafez EE (2017) Induction of Apoptosis in Human Cancer Cells Through Extrinsic and Intrinsic Pathways by *Balanites aegyptiaca* Furostanol Saponins and Saponin-Coated Silver Nanoparticles. *Appl Biochem Biotechnol* 182(4):1675-1693 doi:10.1007/s12010-017-2426-3
20. El-Readi MZ, Althubiti MA (2019) Cancer Nanomedicine: A New Era of Successful Targeted Therapy. *Journal of Nanomaterials* 2019:4927312 doi:10.1155/2019/4927312
21. Ventola CL (2017) Progress in Nanomedicine: Approved and Investigational Nanodrugs. *P t* 42(12):742-755
22. Rheder DT, Guilger M, Bilesky-José N, Germano-Costa T, Pasquoto-Stigliani T, Gallep TBB, Grillo R, Carvalho CDS, Fraceto LF, Lima R (2018) Synthesis of biogenic silver nanoparticles using *Althaea officinalis* as reducing agent: evaluation of toxicity and ecotoxicity. *Sci Rep* 8(1):12397 doi:10.1038/s41598-018-30317-9
23. Hamouda RA, Hussein MH, Abo-Elmagd RA, Bawazir SS (2019) Synthesis and biological characterization of silver nanoparticles derived from the cyanobacterium *Oscillatoria limnetica*. *Sci Rep* 9(1):13071 doi:10.1038/s41598-019-49444-y
24. Husain S, Afreen S, Hemlata, Yasin D, Afzal B, Fatma T (2019) Cyanobacteria as a bioreactor for synthesis of silver nanoparticles-an effect of different reaction conditions on the size of nanoparticles and their dye decolorization ability. *Journal of Microbiological Methods* 162:77-82 doi:<https://doi.org/10.1016/j.mimet.2019.05.011>
25. Rosman NSR, Harun NA, Idris I, Ismail WIW (2020) Eco-friendly silver nanoparticles (AgNPs) fabricated by green synthesis using the crude extract of marine polychaete, *Marphysa moribidii*: biosynthesis, characterisation, and antibacterial applications. *Heliyon* 6(11):e05462 doi:10.1016/j.heliyon.2020.e05462
26. Tomer AK, Rahi T, Neelam DK, Dadheech PK (2019) Cyanobacterial extract-mediated synthesis of silver nanoparticles and their application in ammonia sensing. *International Microbiology* 22(1):49-58 doi:10.1007/s10123-018-0026-x

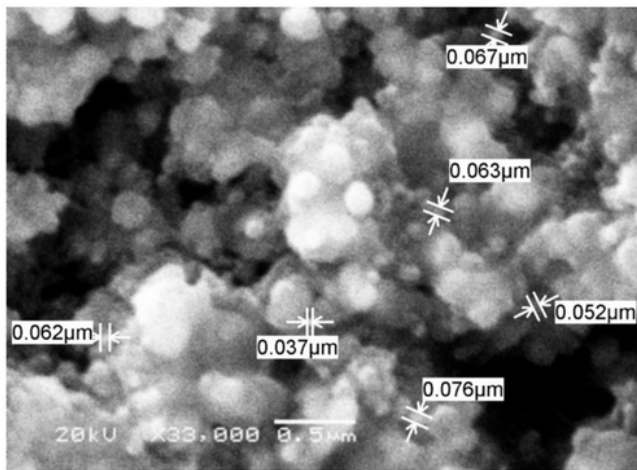
27. Mahdieh M, Zolanvari A, Azimee AS, Mahdieh M (2012) Green biosynthesis of silver nanoparticles by *Spirulina platensis*. *Scientia Iranica* 19(3):926-929 doi:<https://doi.org/10.1016/j.scient.2012.01.010>
28. Sharma A, Sharma S, Sharma K, Chetri SPK, Vashishtha A, Singh P, Kumar R, Rathi B, Agrawal V (2016) Algae as crucial organisms in advancing nanotechnology: a systematic review. *Journal of Applied Phycology* 28(3):1759-1774 doi:10.1007/s10811-015-0715-1
29. Othman AM, Elsayed MA, Al-Balakocy NG, Hassan MM, Elshafei AM (2019) Biosynthesis and characterization of silver nanoparticles induced by fungal proteins and its application in different biological activities. *J Genet Eng Biotechnol* 17(1):8-8 doi:10.1186/s43141-019-0008-1
30. Skandalis N, Dimopoulou A, Georgopoulou A, Gallios N, Papadopoulos D, Tsipas D, Theologidis I, Michailidis N, Chatzinikolaïdou M (2017) The Effect of Silver Nanoparticles Size, Produced Using Plant Extract from *Arbutus unedo*, on Their Antibacterial Efficacy. *Nanomaterials (Basel)* 7(7):178 doi:10.3390/nano7070178
31. Yang EJ, Kim S, Kim JS, Choi IH (2012) Inflammasome formation and IL-1 β release by human blood monocytes in response to silver nanoparticles. *Biomaterials* 33(28):6858-67 doi:10.1016/j.biomaterials.2012.06.016
32. Carnovale C, Bryant G, Shukla R, Bansal V (2019) Identifying Trends in Gold Nanoparticle Toxicity and Uptake: Size, Shape, Capping Ligand, and Biological Corona. *ACS Omega* 4(1):242-256 doi:10.1021/acsomega.8b03227
33. Fratoddi I, Venditti I, Cametti C, Russo MV (2015) How toxic are gold nanoparticles? The state-of-the-art. *Nano Research* 8(6):1771-1799 doi:10.1007/s12274-014-0697-3
34. Gerber A, Bundschuh M, Klingelhofer D, Groneberg DA (2013) Gold nanoparticles: recent aspects for human toxicology. *Journal of Occupational Medicine and Toxicology* 8(1):32 doi:10.1186/1745-6673-8-32
35. Hornos Carneiro MF, Barbosa F (2016) Gold nanoparticles: A critical review of therapeutic applications and toxicological aspects. *Journal of Toxicology and Environmental Health, Part B* 19(3-4):129-148 doi:10.1080/10937404.2016.1168762
36. Ferdous Z, Nemmar A (2020) Health Impact of Silver Nanoparticles: A Review of the Biodistribution and Toxicity Following Various Routes of Exposure. *Int J Mol Sci* 21(7) doi:10.3390/ijms21072375
37. Patlolla AK, Hackett D, Tchounwou PB (2015) Silver nanoparticle-induced oxidative stress-dependent toxicity in Sprague-Dawley rats. *Mol Cell Biochem* 399(1-2):257-68 doi:10.1007/s11010-014-2252-7
38. Ashraf JM, Ansari MA, Khan HM, Alzohairy MA, Choi I (2016) Green synthesis of silver nanoparticles and characterization of their inhibitory effects on AGEs formation using biophysical techniques. *Sci Rep* 6:20414 doi:10.1038/srep20414
39. Swanner J, Mims J, Carroll DL, Akman SA, Furdul CM, Torti SV, Singh RN (2015) Differential cytotoxic and radiosensitizing effects of silver nanoparticles on triple-negative breast cancer and non-triple-negative breast cells. *Int J Nanomedicine* 10:3937-53 doi:10.2147/ijn.S80349
40. Fahrenholtz CD, Swanner J, Ramirez-Perez M, Singh RN (2017) Heterogeneous Responses of Ovarian

41. Liu P, Huang Z, Chen Z, Xu R, Wu H, Zang F, Wang C, Gu N (2013) Silver nanoparticles: a novel radiation sensitizer for glioma? *Nanoscale* 5(23):11829-36 doi:10.1039/c3nr01351k
42. Locatelli E, Naddaka M, Uboldi C, Loudos G, Fragogeorgi E, Molinari V, Pucci A, Tsoதாகos T, Psimadas D, Ponti J, Franchini MC (2014) Targeted delivery of silver nanoparticles and alisertib: in vitro and in vivo synergistic effect against glioblastoma. *Nanomedicine (Lond)* 9(6):839-49 doi:10.2217/nnm.14.1
43. Miura N, Shinohara Y (2009) Cytotoxic effect and apoptosis induction by silver nanoparticles in HeLa cells. *Biochem Biophys Res Commun* 390(3):733-7 doi:10.1016/j.bbrc.2009.10.039
44. Kawata K, Osawa M, Okabe S (2009) In vitro toxicity of silver nanoparticles at noncytotoxic doses to HepG2 human hepatoma cells. *Environ Sci Technol* 43(15):6046-51 doi:10.1021/es900754q
45. Sanpui P, Chattopadhyay A, Ghosh SS (2011) Induction of apoptosis in cancer cells at low silver nanoparticle concentrations using chitosan nanocarrier. *ACS Appl Mater Interfaces* 3(2):218-28 doi:10.1021/am100840c
46. Beer C, Foldbjerg R, Hayashi Y, Sutherland DS, Autrup H (2012) Toxicity of silver nanoparticles - nanoparticle or silver ion? *Toxicol Lett* 208(3):286-92 doi:10.1016/j.toxlet.2011.11.002
47. Zielinska E, Zauszkiewicz-Pawlak A, Wojcik M, Inkielewicz-Stepniak I (2018) Silver nanoparticles of different sizes induce a mixed type of programmed cell death in human pancreatic ductal adenocarcinoma. *Oncotarget* 9(4):4675-4697 doi:10.18632/oncotarget.22563
48. Guo D, Zhao Y, Zhang Y, Wang Q, Huang Z, Ding Q, Guo Z, Zhou X, Zhu L, Gu N (2014) The cellular uptake and cytotoxic effect of silver nanoparticles on chronic myeloid leukemia cells. *J Biomed Nanotechnol* 10(4):669-78 doi:10.1166/jbn.2014.1625
49. Guo D, Zhu L, Huang Z, Zhou H, Ge Y, Ma W, Wu J, Zhang X, Zhou X, Zhang Y, Zhao Y, Gu N (2013) Anti-leukemia activity of PVP-coated silver nanoparticles via generation of reactive oxygen species and release of silver ions. *Biomaterials* 34(32):7884-94 doi:10.1016/j.biomaterials.2013.07.015
50. Sriram MI, Kanth SB, Kalishwaralal K, Gurunathan S (2010) Antitumor activity of silver nanoparticles in Dalton's lymphoma ascites tumor model. *Int J Nanomedicine* 5:753-62 doi:10.2147/ijn.S11727
51. Orta-García ST, Plascencia-Villa G, Ochoa-Martínez AC, Ruiz-Vera T, Pérez-Vázquez FJ, Velázquez-Salazar JJ, Yacamán MJ, Navarro-Contreras HR, Pérez-Maldonado IN (2015) Analysis of cytotoxic effects of silver nanoclusters on human peripheral blood mononuclear cells 'in vitro'. *J Appl Toxicol* 35(10):1189-99 doi:10.1002/jat.3190
52. M JF, P L (2015) Apoptotic efficacy of biogenic silver nanoparticles on human breast cancer MCF-7 cell lines. *Prog Biomater* 4(2-4):113-121 doi:10.1007/s40204-015-0042-2
53. Vakkala M, Pääkkö P, Soini Y (1999) Expression of caspases 3, 6 and 8 is increased in parallel with apoptosis and histological aggressiveness of the breast lesion. *Br J Cancer* 81(4):592-9 doi:10.1038/sj.bjc.6690735
54. Mukherjee P, Ahmad A, Mandal D, Senapati S, Sainkar SR, Khan MI, Parishcha R, Ajaykumar PV, Alam Loading [MathJax]/jax/output/CommonHTML/jax.js mediated Synthesis of Silver Nanoparticles and Their

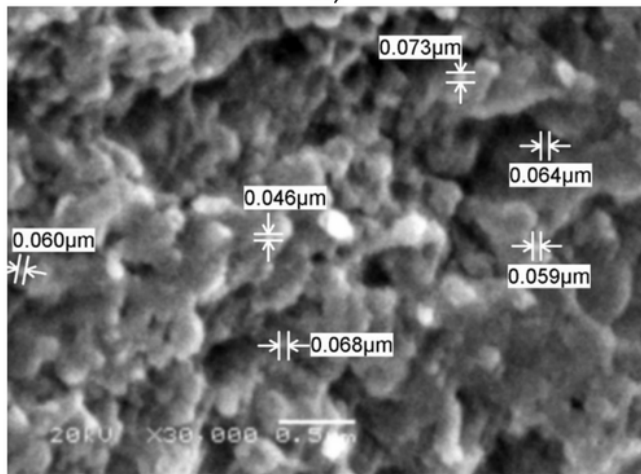
Immobilization in the Mycelial Matrix: A Novel Biological Approach to Nanoparticle Synthesis. *Nano Letters* 1(10):515-519 doi:10.1021/nl0155274

55. Urbańska K, Pająk B, Orzechowski A, Sokołowska J, Grodzik M, Sawosz E, Szmidt M, Sysa P (2015) The effect of silver nanoparticles (AgNPs) on proliferation and apoptosis of in ovo cultured glioblastoma multiforme (GBM) cells. *Nanoscale Res Lett* 10:98 doi:10.1186/s11671-015-0823-5
56. Inwald EC, Klinkhammer-Schalke M, Hofstädter F, Zeman F, Koller M, Gerstenhauer M, Ortmann O (2013) Ki-67 is a prognostic parameter in breast cancer patients: results of a large population-based cohort of a cancer registry. *Breast Cancer Res Treat* 139(2):539-52 doi:10.1007/s10549-013-2560-8
57. Scholzen T, Gerdes J (2000) The Ki-67 protein: from the known and the unknown. *J Cell Physiol* 182(3):311-22 doi:10.1002/(sici)1097-4652(200003)182:3<311::Aid-jcp1>3.0.Co;2-9.

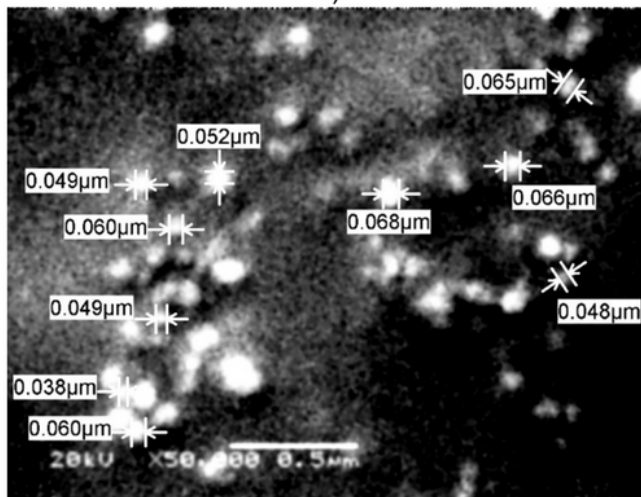
Figures



A)



B)



C)

Figure 1

Scanning electron microscopy image of green synthesized AgNPs. A) AgNPs biosynthesized by *C. vulgaris* cell free supernatant (C-bio-AgNPs), B) AgNPs biosynthesized by *M. aeruginosa* cell free supernatant (M-bio-AgNPs) and C) AgNPs biosynthesized by *Arthrospira platensis* cell free supernatant (A-bio-AgNPs).

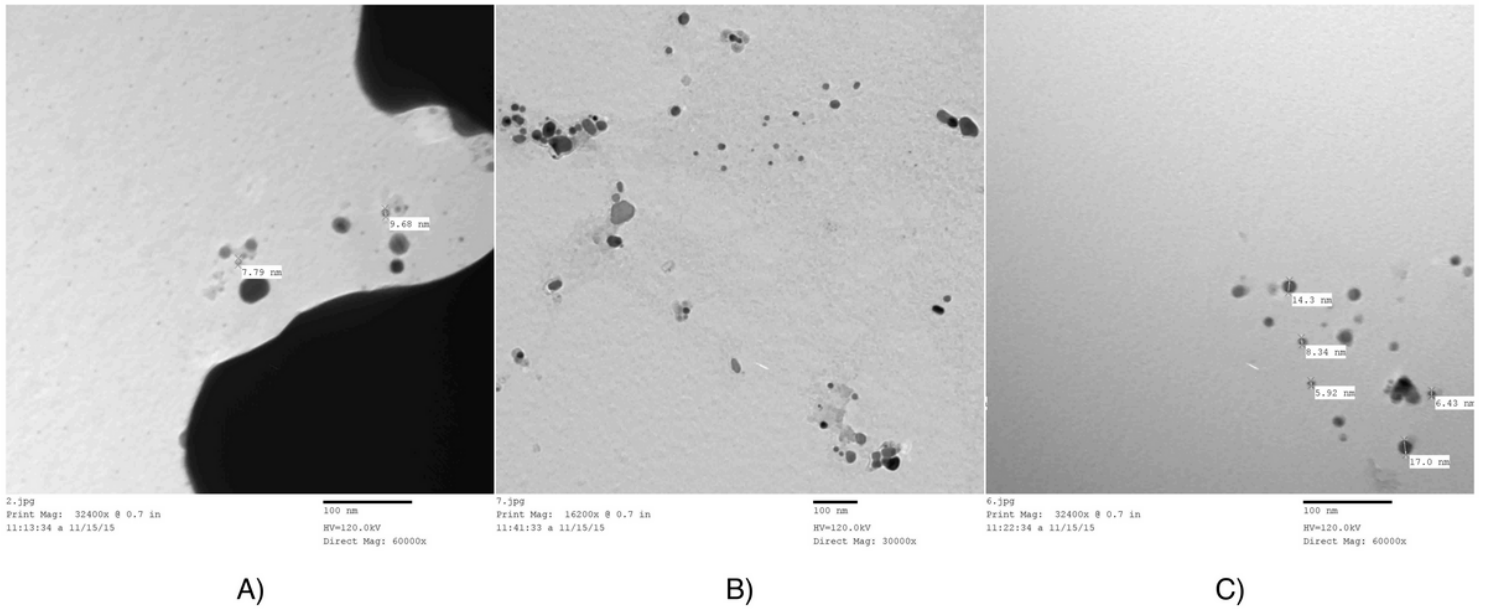


Figure 2

Transmission electron microscopy image of green synthesized AgNPs. A) AgNPs biosynthesized by *C. vulgaris* cell free supernatant (C-bio-AgNPs), B) AgNPs biosynthesized by *M. aeruginosa* cell free supernatant (M-bio-AgNPs) and C) AgNPs biosynthesized by *Arthrospira platensis* cell free supernatant (A-bio-AgNPs).

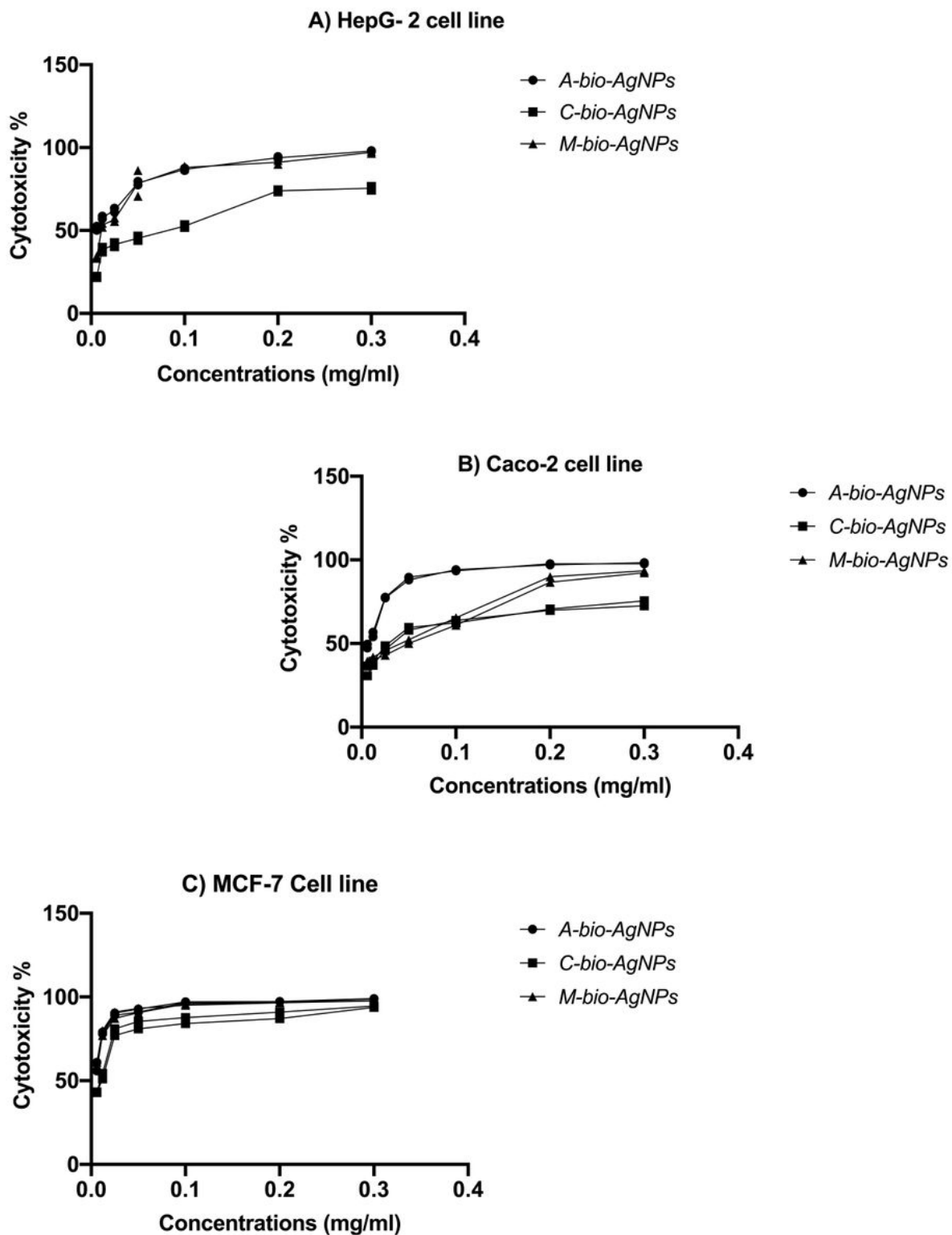


Figure 3

The Anticancer activity of the bio-AgNPs. The anticancer activity of the C-bio-AgNPs, M-bio-AgNPs and A-bio-AgNPs were quantified using MTS using different treatment concentrations against: A) HepG-2 cell line, B) CaCO-2 cell line and C) MCF-7 cell line.

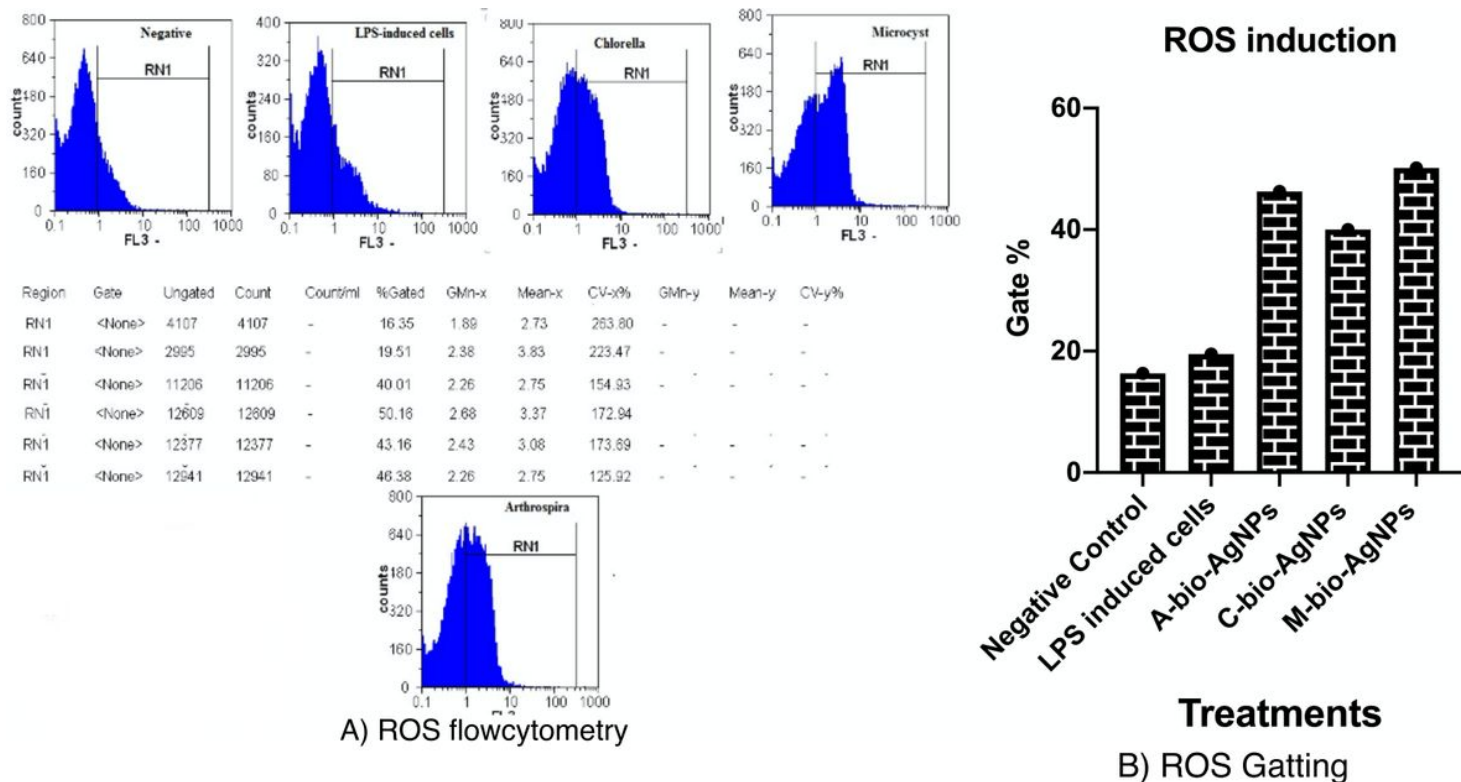


Figure 4

The intracellular reactive oxygen species induced after AgNPs treatment. The induced ROS in PBMCs inflammatory models were quantified after C-bio-AgNPs, M-bio-AgNPs and A-bio-AgNPs treatment using IC50 concentrations. The induced ROS were quantified using H2DCF-DA and flowcytometry, the results were expressed as Gating % after H2DCF-DA and compared with the LPS- induced PBMCs (lipopolysaccharide 100 ng/ml).

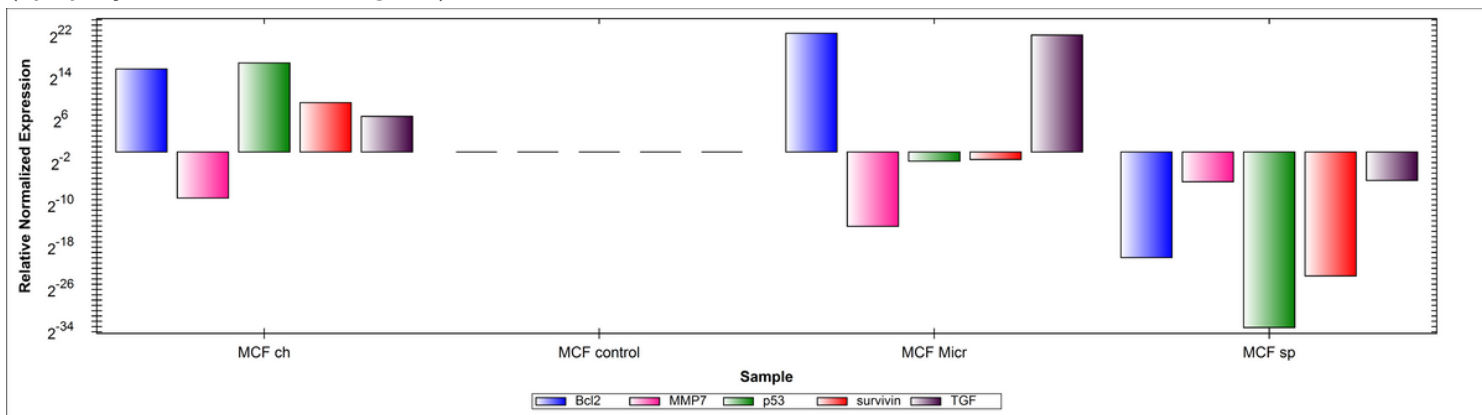
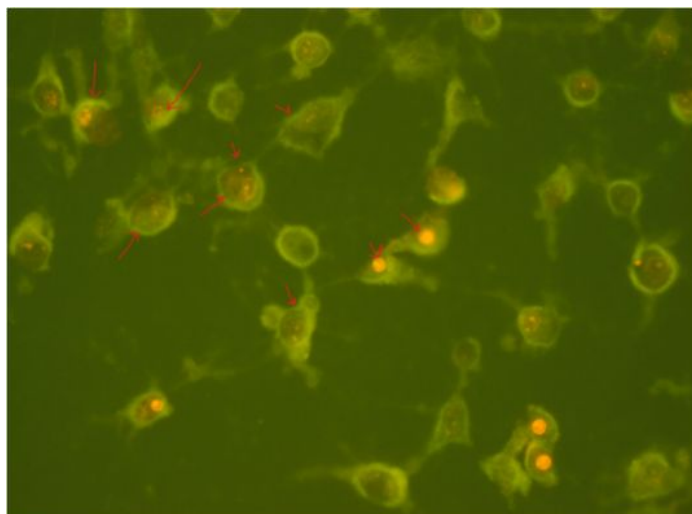
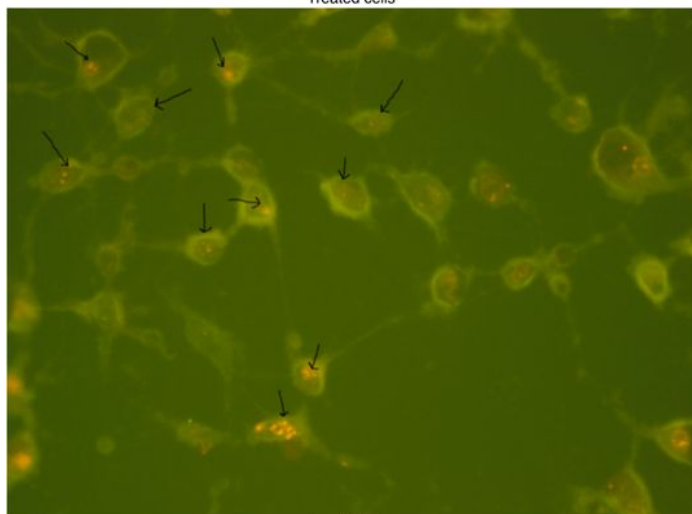


Figure 5

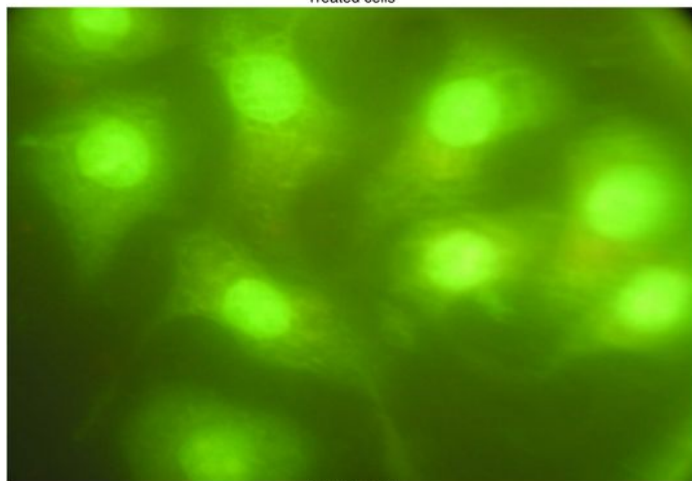
The regulatory effects of A-bio-AgNPs treatment on oncogenes and tumor suppressor genes. The regulatory effects of A-bio-AgNPs on p53, Bcl2, MMP7 (metalloproteinase 7), TGFα (Transforming growth factor) and Survivin genes were quantified after 24hrs treatments with sub-IC50 concentrations using RTqPCR.



Treated cells



Treated cells



Control cells

Figure 6

Induction of apoptosis and necrosis after A-bio-AgNPs treatment. MCF7 cancer cells treated with A-bio-AgNPs IC50 concentration. Arrows indicate early apoptotic cells and multinucleated cells, cells with condensed nucleus and necrotic staged cells.

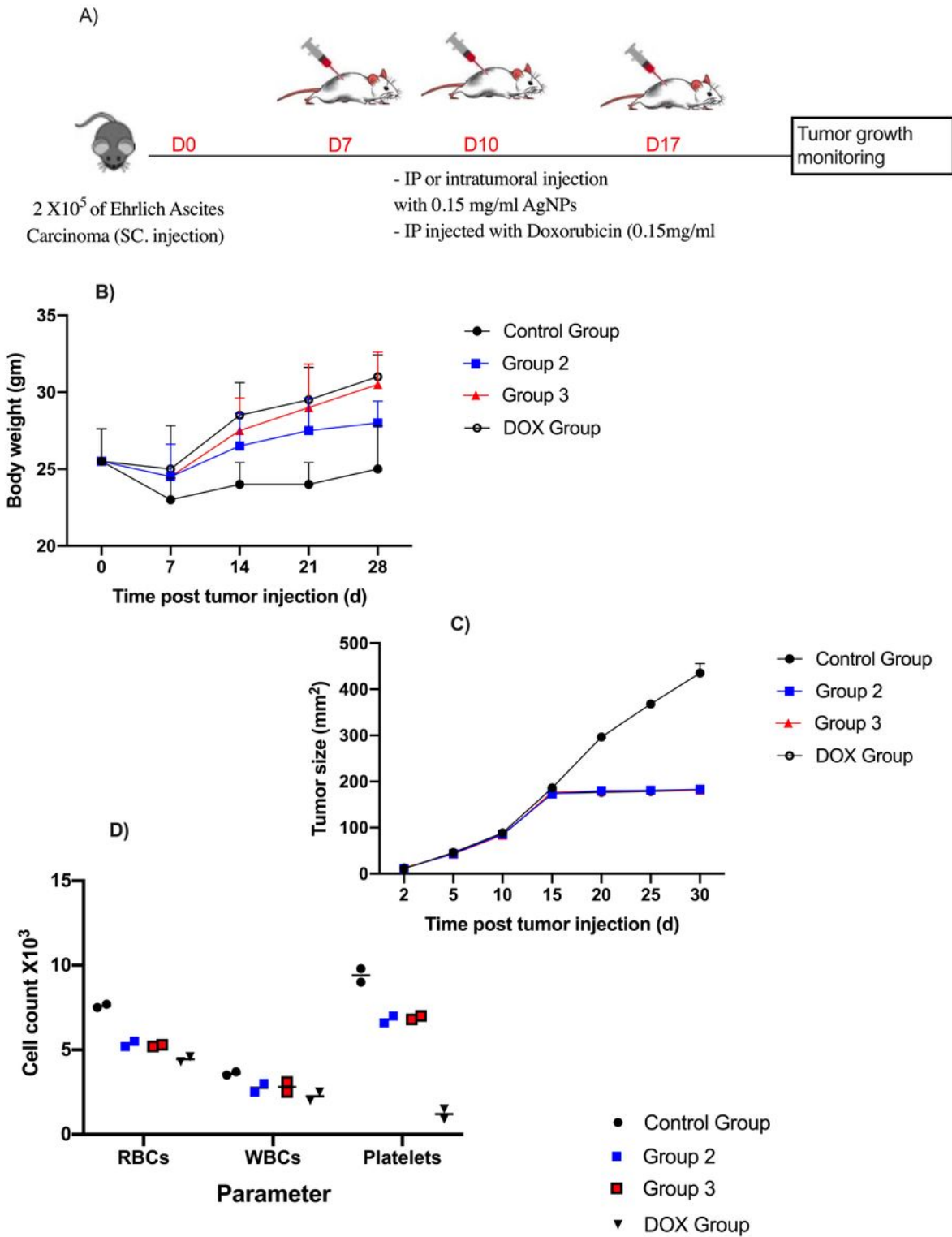


Figure 7

The control of breast cancer growth using A-bio-AgNPs in vivo Body weight (A) and tumor size (B) Platelets, WBCs and RBCs counts that recorded over 28 days in three groups of tumors bearing females BALB/C mice (each group have 5 mice). Group 1: Negative control mice; mice were IP injected with 9% saline. Group 2: Mice were injected locally (intertumoral injections) with 0.15mg/ml of A-bio- Loading [MathJax]/jax/output/CommonHTML/jax.js Mice were injected intraperitoneally with 0.15mg/ml of A-bio-

AgNPs (3.5gm/Kg body weight). DOX group: mice were IP injected with Doxorubicin (DOX; 0.15mg/ml; 3.5gm/Kg body weight).

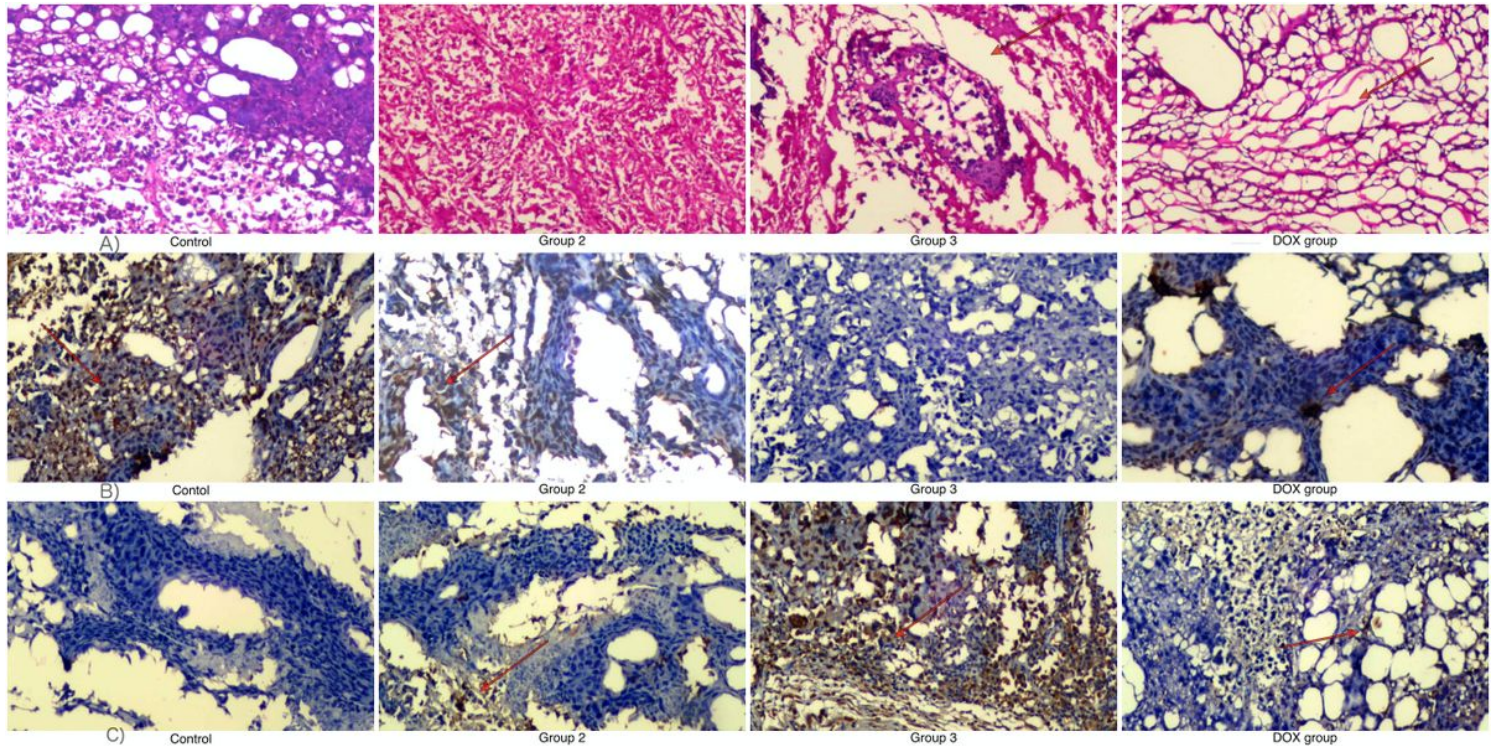


Figure 8

Histopathology and Immunohistochemistry staining sections of breast tumor and adjacent stroma from individual. The upper 4 figure showed the histopathological staining with (H&E), examined microscopically for presence of negative features, such as edema, erosion and necrosis. The second 4 figures in the middle showed the Immunohistochemistry staining of Ki 67 protein and the lower 4 figures represent Immunohistochemistry staining of caspase 3 protein. (a) Negative control mice; mice were IP injected with 9% saline, (b) Mice were injected locally (intertumoral injections) with 0.15mg/ml of A-bio-AgNPs (3.5gm/Kg body weight), (c) mice were injected intraperitoneally with 0.15mg/ml of A-bio-AgNPs (3.5gm/Kg body weight), (d) mice were IP injected with Doxorubicin (DOX; 0.15mg/ml; 3.5gm/Kg body weight).

Supplementary Files

This is a list of supplementary files associated with this preprint. Click to download.

- [graphicalabstract.png](#)
- [Supplementaryfile.docx](#)